Int. J. Multiphase Flow, Vol. 5, pp. 59–78. Pergamon/Elsevier, 1979. Printed in Great Britain

DISPERSION IN ANNULAR CLIMBING FILM FLOW

A. ROUKENS DE LANGE

Department of Chemical Engineering, University of the Witwatersrand, Johannesburg, 2001 South Africa

(*Received* 16 *November* 1976; *accepted* 17 *August* 1978)

Abstract—The dispersion of a tracer injected as a pulse into a climbing liquid film is investigated for a series of water and air flow rates, and for a number of different electrolyte tracers. It is found that at all flow rates the observed concentration distribution depends on the nature of the tracer. This observation is explained in terms of two effects: molecular diffusion in a viscous sub-layer and ion fractionation associated with droplet formation at the gas–liquid interface. The overall dispersive characteristics of the system are described in terms of a mathematical model assuming dispersed plug flow in both the film and entrained droplets with interchange between these phases. This model is fitted to experimental tracer concentration distributions using a non-linear least-squares regression procedure. The parameter values obtained from the fitting procedure are studied to determine trends with flow rates and tracer properties. Values for a film dispersion parameter, P_f, are found to correlate significantly with the molecular diffusion coefficients of the tracers. Consistent values for an ion fractionation coefficient, k_{if}, are also obtained.

1. INTRODUCTION

The characteristics of annular two-phase flow have been extensively investigated by numerous researchers. Much of this work has been digested and put in perspective by Hewitt & Hall-Taylor (1970) in an excellent book on this topic. The investigation reported here mainly concerns the analysis of the concentration distribution resulting from the dispersion of a pulse of tracer. The flow regime investigated is that of climbing film flow, i.e. vertical upward annular two-phase flow. The topic of dispersion in annular climbing film flow is not dealt with by Hewitt and Hall-Taylor and the only known earlier work in this field is that by Jagota *et al.* (1972, 1973*a*).

The dispersion of a tracer in a flow system results from randomising influences in the system. It follows that the concentration distribution recorded downstream from a tracer injection point will contain implicit information about these randomising influences. With proper mathematical handling of the concentration distribution data this information may be extracted in the form of parameters characterising the flow. In single-phase one-dimensional flow, the major dispersive effects are molecular diffusion, turbulent eddies, and the velocity profile. The dispersive behaviour observed in this simple flow situation has been adequately interpreted from theoretical considerations by several authors, e.g. Taylor (1953), Aris (1956) and Gill & Sankarasubramanian (1971). A much more complex set of physical factors gives rise to the dispersion patterns observed in annular climbing film flow. In addition to the factors indicated for the single phase flow situation, several other effects are involved. A complex pattern of waves and turbulence exists at the interface between the two phases, and a characteristic feature is that of disturbance waves which act as the source of entrainment (Hewitt & Hall-Taylor 1970). Entrained droplets carrying tracer material are thus constantly breaking away from the film, to be redeposited later out of the gas core. In this paper we shall be concerned with the acquisition of dispersion data and the analysis of such data to obtain information on the various dispersive effects in the annular climbing film flow regime.

2. EXPERIMENTAL PROCEDURE

The climbing film apparatus used was very similar in principle to that used by numerous other investigators (Jagota *et al.* 1973*a*,*b*; Roberts 1969). Filtered and saturated air were led, after metering, to the bottom of a 34 mm I.D. Perspex tube. The entrance section was arranged as shown diagrammatically in figure 1. Pressure in the tube was regulated at a constant value of

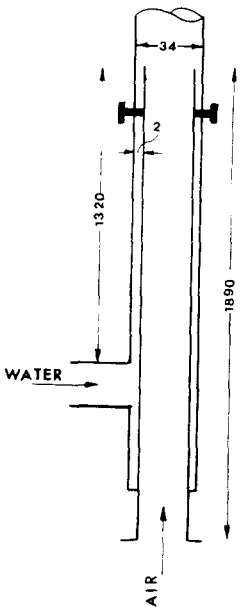

Figure 1. Entrance section to climbing film tube.
Dimensions in mm (not to scale).

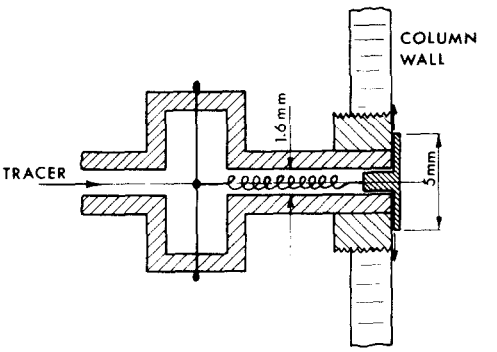

Figure 2. Construction of injection nozzle.

164 kN m^{-2} at the midpoint of the test section. A tracer injection point was situated 3.9 m above the point of first contact between gas and liquid. Tracer concentration distributions were measured using conductance cell probes at heights of 3 and 6 m above the injection point. Pressure and disturbance wave frequency and velocity were measured in a manner similar to that described by Hewitt *et al.* (1964).

Tracer injections were made as follows. Four pipetting syringes were fixed in parallel on a board. A bar resting against the plungers was mounted such that it could be depressed a preset distance to deliver equal quantities of tracer from each syringe. Four injection points were drilled at 90° to one another at the same vertical level on the column and each of these points was connected to a syringe outlet. To prevent the tracer from being squirted through the film and into the core a special injection nozzle was designed. The construction of this nozzle is illustrated in figure 2. A very fine phosphor–bronze hair spring was fitted inside a length of 1.6 mm I.D. stainless steel tube. At one end the spring was attached to a fixed pin while at the other end the spring was attached to a circular cap. When the syringe plunger was depressed the pressure in the tube forced out the cap, and liquid could escape radially outwards in the space between the cap and the sleeve which screwed into the column wall. The quantity injected could be varied to give the desired signal level at the conductivity measurement point, a typical quantity being 0.3 cm^3 per syringe.

Tests carried out to establish the effect of an obstruction in the tube wall indicated that its effect on the concentration distribution further up the tube was negligible so that the influence of the caps in the film could be ignored. On the other hand the injection of tracer at more than one point on the circumference was found to be essential. Experiments in which a dye was injected continuously at a point in the film indicated that tracer injected at a point would only begin to reach the opposite side of the tube by a process of circumferential dispersion at a distance of the order of 2 m beyond the injection point. Dispersion by entrainment and redeposition was, however, much faster (see Section 5).

To measure the conductance of the liquid without influence from variations in film thickness, a special conductance cell probe was developed as illustrated in figure 3. Two short lengths of platinum wire, about 150 μm in diameter, were threaded down a 1 mm I.D. stainless steel tube and fixed in this tube by a small amount of dental impression wax. Previously the

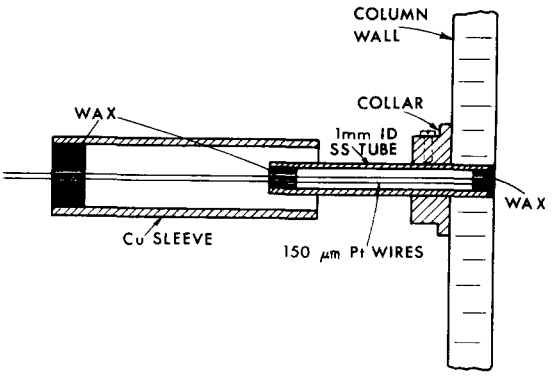

Figure 3. Construction of conductance probe.

platinum wire had been sprayed with a coating of insulating shellac. The cross-sectional surfaces of the platinum wires, exposed in the squared-off end of the tip, formed the electrodes. To provide some robustness for the cell, the end of the stainless steel tube and the wires protruding from it were fixed into a short length of copper tube by means of impression wax. The tube carrying the platinum wires fitted smoothly through a hole in the climbing film tube wall. The tip of the probe was allowed to penetrate into the wall until it was almost flush with the inner wall. Any penetration beyond the inner wall surface gave rise to a noisy response from the probe due to the effect of variable film thickness. The same probe was also used to measure concentration distributions in the droplets of the core. In this case the probe was allowed to penetrate into the centre of the tube. A continuous stream of droplets was relied upon to keep the tip of the probe constantly wetted.

In order to obtain a reproducible response from the conductance probe and a linear relationship between concentration and conductance, it proved to be essential to plate the exposed tips of the platinum wire with platinum black, and to use distilled water and very low tracer concentrations. Deviations from linearity for all electrolytes used were found to be less than 2% at peak tracer concentrations of 150 p.p.m.

The conductance of the liquid flowing over a conductance cell probe was measured by means of a Wayne Kerr Autobalance Universal bridge, adapted to give a nearly instantaneous though slightly underdamped response. Deviations from linearity between input and output from the bridge were undetectably small. The output signal was passed through a filter set to remove noise of frequency greater than 20 Hz, and recorded on an instrumentation tape recorder. The recorded signal was later digitised to provide a magnetic tape which could be processed by a computer. The operation of the digitising system used has been described by Green (1973).

Further details of the equipment, measuring instruments and experimental procedures may be found in the present author's doctoral thesis (Roukens de Lange, 1975).

3. EXPERIMENTAL RESULTS

Dispersion measurements were made for five different combinations of air and water rates. These flow rates covered a fairly typical range of gas and liquid flow conditions, but no very high liquid or low gas rates. The mean experimental conditions for each combination of flow rates are given in table 1. For each experiment (i.e. set of gas and liquid rates) the impulse response for tracers HNO_3, KCl, KOH, LiCl and $MgSO_4$ were measured in triplicate in both the film and the core. These electrolytes were chosen in order to cover a wide range of molecular diffusivity.

Table 1. Experimental conditions for dispersion measurements. Experimental code identifies gas flow rate (B, C and D) and liquid flow rate (1, 2 or 3) W is mass flow rate, Re is Reynolds number, t is temperature, $|\Delta P/\Delta z|$ is pressure gradient, f_w and u_w are disturbance wave frequency and velocity. Subscripts L and G represent liquid and gas respectively

Experiment	W_L ($kg\,s^{-1} \times 10^3$)	Re_L	W_G ($kg\,s^{-1} \times 10^3$)	Re_G	t (°C)	$\lvert\Delta P/\Delta z\rvert$ ($N\,m^{-3}$)	f_w (s^{-1})	u_w ($m\,s^{-1}$)
B2	15.0	547	38.8	79,000	19.4	700	5.7	1.99
C1	5.0	188	55.4	113,000	21.8	780	—	—
C2	15.0	524	55.4	113,000	18.7	1170	7.9	2.62
C3	45.0	1840	55.4	113,000	25.4	1650	13.1	3.23
D2	15.0	576	83.2	170,000	22.8	2100	10.4	3.66

The effect of gas and liquid flow rate on the observed concentration distribution is shown in figure 4(i). The tracer used in all these runs was KCl. The effect of the tracer for a typical set of flow rates is shown clearly in figure 4(ii). An example of concentration distributions obtained in the core is shown in figure 4(iii). Here the effect of tracer is not so obvious and a lot of noise is evident as a result of uneven wetting of the probe. In figure 4(iv) the reproducibility of results is illustrated. More experimental concentration distributions may be found elsewhere (Roukens de Lange, 1975).

It is clear from figure 4(i) that the dispersion pattern is strongly influenced by flow rate. Not only is the spread increased with both increasing gas and liquid rates, but the shape of the curves is changed. The spreading and skewing trends agree with the trends that would be expected as a result of the known increase in entrainment and redeposition of droplets with increasing gas and liquid rates (Gill *et al.* 1964; Cousins & Hewitt 1968*a*).

From the results given in figure 4(ii) it can be seen that the falling slope becomes steeper in the order $MgSO_4$, LiCl, KCl, KOH, HNO_3. A similar though not always totally consistent effect was observed for other experimental conditions. A much stronger effect occurs in the rising slope. Here slopes for tracers HNO_3 and KOH rise later and faster than slopes for the other tracers. This behaviour was observed consistently except in the case of Experiment C1 in which no entrainment occurred.

For a truly viscous laminar film the dispersion theory of Taylor (1953) and Aris (1956) indicates that the concentration distribution resulting from an impulse injection should be normally distributed with a variance inversely proportional to D_{mol}, the molecular diffusion coefficient value of the tracer material. In table 2, values of D_{mol} for the tracers used are given and it can be seen that the trend observed in the falling slopes is the same, though less pronounced, as would be expected for dispersion in a viscous film. This observation can probably be explained by postulating the existence of a very thin continuous viscous sub-layer next to the tube wall. In the rest of the film any molecular diffusion effect will be totally swamped by the large amount of turbulence generated as a result of ripple and disturbance waves at the gas–liquid interface (Hewitt 1969).

The tracer dependent effect in the rising slope of the concentration distribution is more difficult to interpret. Interpretations based on molecular diffusivity or modifications of bulk or interfacial properties due to the tracer material are highly improbable and electrolyte concen-

Table 2. Values for molecular diffusion coefficients, D_{mol}, at 25°C and infinite dilution

Tracer	D_{mol} ($m^2\,s^{-1} \times 10^9$)
HNO_3	3.122
KOH	2.858
KCl	1.993
LiCl	1.366
$MgSO_4$	0.849

trations are so low that surface tension and viscosity are essentially unaffected. An experiment was carried out to determine the adsorption of ions on Perspex in order to investigate the possibility of a chromatographic effect at the tube wall, but no adsorption could be detected. An interpretation can, however, be given in terms of the phenomenon of ion fractionation. It has been known for some time that the distribution of ions in sea spray is different from that in sea water (Symposium on Sea–Air Chemistry 1972). The phenomenon is ascribed to an ion concentration effect at an interface, the relative magnitude of which varies from one ion to another. To date no satisfactory mechanism appears to have been advanced to explain this effect. MacIntyre (1972, 1974) has investigated the phenomenon of ion fractionation by studying spray formation at a water–air interface. He found that when a typical bubble of 1 mm diameter breaks, a couple of larger jet drops (20–100 μm) and some very fine spray droplets (1–20 μm)

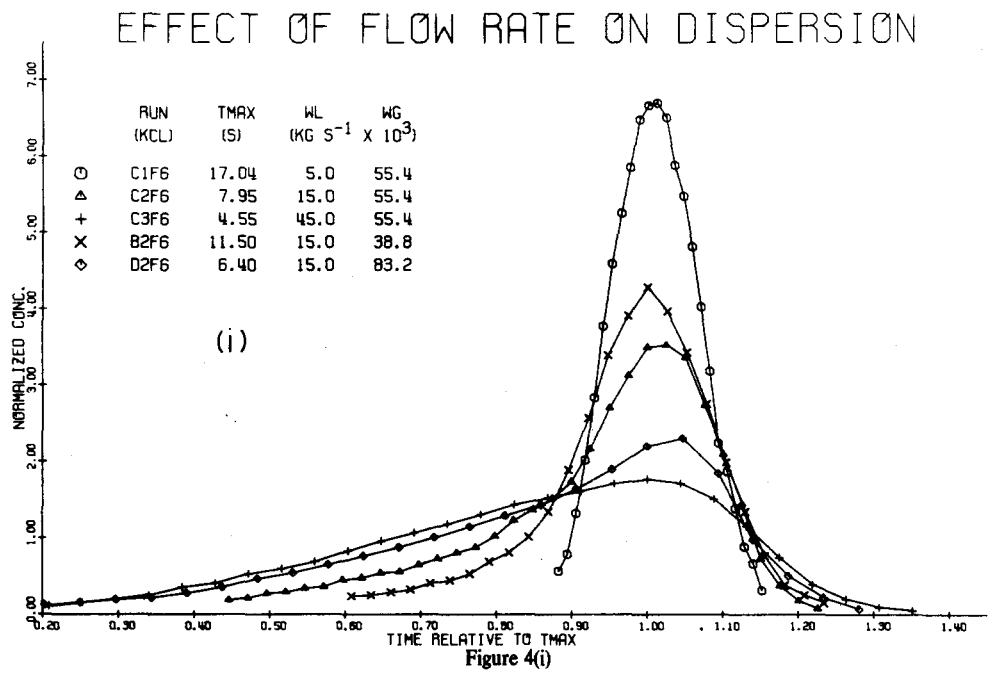

Figure 4(i)

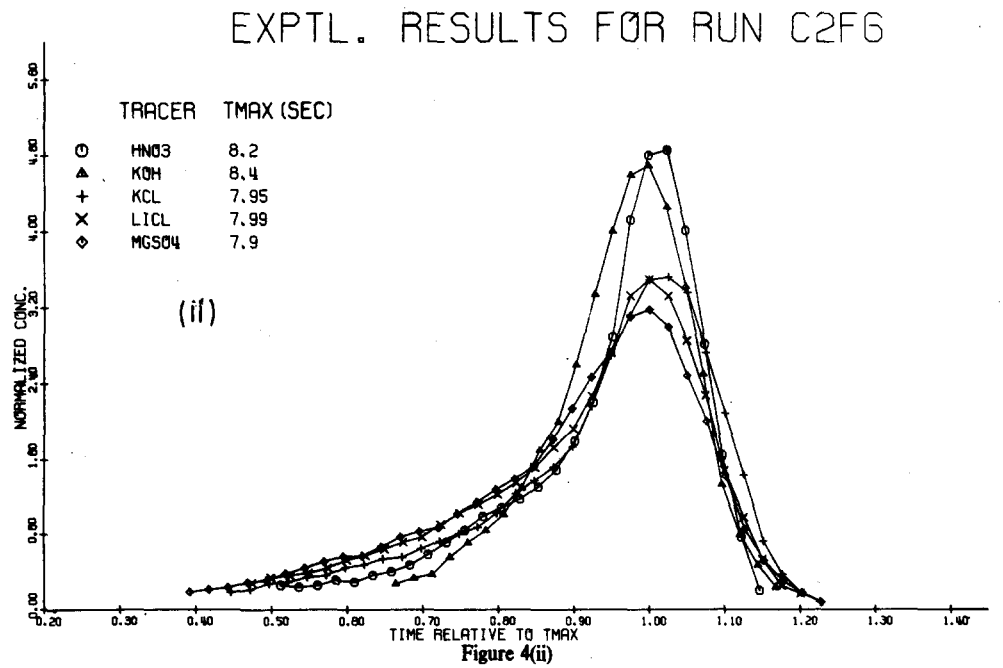

Figure 4(ii)

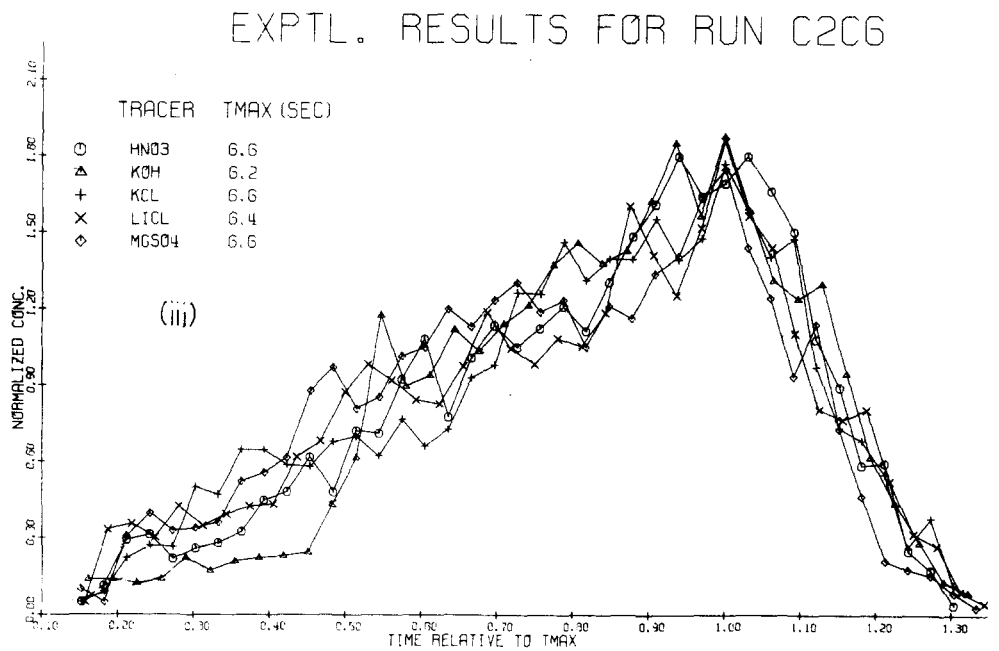

Figure 4(iii)

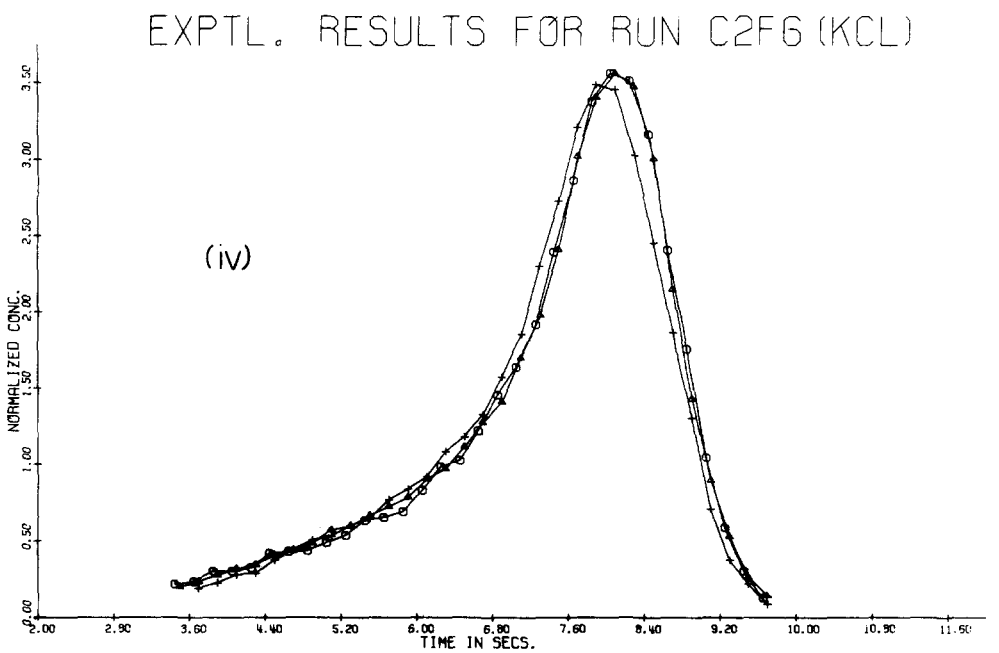

Figure 4(iv)

Figure 4. Experimental dispersion results. Runs are identified by a 4-symbol alphameric code. The first two symbols indicate the flow conditions for the run, as in table 1. The third symbol indicates whether the concentration distribution was measured in the film (F) or in the dispersed phase in the core (C). The last symbol indicates whether the measurement was made at a height of 6.12 m (6) or 3.05 m (3) above the injection point. The key heading T_{max} indicates the time at which the maximum experimental concentration was recorded. Time values along the abscissa have been scaled relative to T_{max}. Concentration values have been scaled to give normalised concentration distributions.

are formed. The liquid contained in all these droplets appears to be made up of surface material extending only about 0.05% of the bubble diameter below the interface.

To test whether ion fractionation does in fact occur in climbing film flow, an experiment was

carried out in which a mixture of ions was injected continuously at a point in the film. Samples of film material were withdrawn at points higher up the tube but diametrically opposite the injection point. The idea behind this experiment was that at heights below that at which tracer has reached the opposite side of the tube by circumferential dispersion through the film itself, any tracer that is detected must have reached the sampling point by entrainment and subsequent deposition. If ion fractionation occurs this will result in a different proportion of ions in entrained and redeposited droplets, and hence in the film samples, than existed in the tracer injected.

The tracer mixture that was used consisted of a mixture of HCl, $CuCl_2$, $MgCl_2$, KCl and LiCl. Samples of the liquid film were analysed for the metal ions by atomic absorption (AA) spectrophotometry. Acid concentratiion was measured by titration with KOH. In table 3 the results obtained are presented as the ratio $r_c = c_f/c_m$ of film sample concentration to the mixed sample concentration. This mixed sample was obtained after the tracer had mixed homogenerously with all the liquid flowing in the tube. Values are also given for R_c, the ratio of r_c for any particular ion to the value of r_c for the hydrogen ion. The results are rather scattered as a result of the poor precision of AA spectrophotometry as a method of analysis. It is nonetheless clear from these results that ion fractionation does indeed occur and that the hydrogen ion has a much lower relative concentration in entrained droplets, and hence at the interface, than the other ions.

Table 3. Results of test for ion fractionation by continuous tracer injection

Height	H^+	Cu^{2+}		Mg^{2+}		Li^+		K^+	
(m)	r_c	r_c	R_c	r_c	R_c	r_c	R_c	r_c	R_c
0.6	0.0017	0.0038	2.24	—	—	0.0062	3.62	—	—
0.8	0.0080	0.0123	1.54	0.0128	1.59	0.0138	1.72	0.0142	1.77
1.0	0.0181	0.0292	1.61	0.0241	1.33	0.0260	1.44	0.0250	1.38
1.2	0.0352	0.0461	1.25	0.0429	1.22	0.0432	1.19	0.0410	1.16
1.4	0.0525	0.0708	1.35	0.0730	1.39	0.0630	1.20	0.0606	1.15
1.6	0.0816	0.1039	1.27	0.0979	1.20	0.0960	1.18	0.1010	1.24
2.0	0.1440	0.1871	1.30	0.1666	1.16	0.1646	1.14	0.1582	1.10
2.4	0.2900	0.3643	1.26	0.3219	1.11	0.3212	1.11	0.3079	1.06

4. THEORETICAL DEVELOPMENT

Interchange dispersion model (IDM)

A mathematical model describing dispersion in annular climbing film flow must be capable of accounting for the major features brought out in the experimental investigation in terms of physically realistic considerations. Such a model is developed elsewhere (Roukens de Lange 1978). Further details are given in the author's doctoral thesis (1975). A bare outline of the model and the results obtained using it in the interpretation of experimental results will be presented here.

The model describes dispersion by independent dispersed plug flow models (DPFMs) in both the film and entrained phases. Allowing for interchange of material between these phases, a mass balance for the system results in the equations

$$\frac{\partial C_f}{\partial T} + U_f \frac{\partial C_f}{\partial Z} - \frac{1}{P_f}\frac{\partial^2 C_f}{\partial Z^2} + J_f U_f (C_f - C_d/k_{if}) = 0 \qquad [1a]$$

and

$$\frac{\partial C_d}{\partial T} + U_d \frac{\partial C_d}{\partial Z} - \frac{1}{P_d}\frac{\partial^2 C_f}{\partial Z^2} + J_d U_d (C_d - k_{if} C_f) = 0 \qquad [1b]$$

where C is a dimensionless concentration, c/c_m; U is a dimensionless velocity, u/u_m; Z is a dimensionless distance along the tube axis, z/l; P is a dimensionless dispersion parameter, $u_m l/D$; k_{if} is an ion fractionation coefficient; l is a characteristic length used in defining dimensionless quantities and is usually set at $1m$; D is a diffusion or dispersion coefficient; subscripts f, d and m refer to film, dispersed or droplet phase, and mean conditions respectively; and

$$J_f = \frac{Ilk_{if}}{1-E} \qquad [2a]$$

and

$$J_d = \frac{Il}{E} \qquad [2b]$$

where I is the fraction of total liquid flow interchanged per unit length and E is the fraction of the liquid flow rate entrained in the gas core. This model is known as the *interchange dispersion model* or IDM.

Ion fractionation is allowed for in this model by assuming that the tracer concentration in all entrained droplets is enriched by a factor k_{if} relative to the liquid in the film at the point from which it was entrained.

The justification for the use of the DPFM and hence the IDM is not obvious on physical grounds. The liquid film is not uniform in thickness. It has a viscous sub-layer covered with ripple waves, while disturbance waves, which travel much faster than the rest of the film and appear to roll over it, carry up a considerable proportion of the liquid. The entrained droplets vary over a large range of size and velocity but not necessarily according to the distribution of the DPFM (Hewitt & Hall-Taylor 1970; Hewitt 1969). However, the use of the DPFM can be argued as a corollary to the result, obtained by Aris (1956), that the solution for dispersion in one-dimensional flow will tend to the solution of the DPFM for large time, independent of velocity distribution or the nature of the mixing process. More detailed arguments justifying the use of the DPFM and IDM models are presented elsewhere (Roukens de Lange 1975; 1978).

Effect of viscous sub-layer and disturbance waves

It can be shown that the dispersion parameter, P_f, is given by the expression

$$\frac{1}{P_f} = BP_{\text{mol}} + \frac{Y_i - Y_v}{Y_i P_t} \qquad [3]$$

where

$$B = \frac{Y_v^3}{Y_i - Y_i^2}\left[-\frac{a^2Y_v^3}{8Y_i} + \frac{7aU_tY_v^2}{12Y_i} + \frac{a^2Y_v^2}{20} - \frac{aU_tY_v}{4} + \frac{a^2Y_v^4}{12Y_i^2}\right.$$

$$\left. - \frac{aU_tY_v^3}{3Y_i^2} + \frac{U_t^2}{3} - \frac{2U_t^2Y_v}{3Y_i} + \frac{U_t^2Y_v^2}{3Y_i^2}\right]. \qquad [4]$$

Y_v and Y_i are the thickness of the viscous sub-layer and the mean film thickness respectively. U_t is the ratio u_t/u_m where u_t is the velocity of the turbulent layer of the film (i.e. that part of film flow not in the viscous layer but including the disturbance waves) and u_m is the mean velocity of all the liquid, including entrained droplets. The velocity profile in the viscous sub-layer is given by

$$U_v(Y) = aY \qquad [5]$$

where a may be obtained for any set of experimental flow rates and pressure gradient using a simple momentum balance.

$P_{mol} = u_m l / D_{mol}$ is the dimensionless diffusion coefficient for the viscous layer. P_t is the dispersion coefficient for the turbulent layer. On the basis of a set of assumptions, the main one being that disturbance waves mix completely with the film as they flow past, the following expression for P_t is obtained.

$$\frac{1}{P_t} = \frac{U_t^2}{2F_w}\left[(1-r_u)^2 + \frac{r_u^2}{3}\right]. \qquad [6]$$

Here $F_w = f_w l / u_f$ is the dimensionless disturbance wave frequency, and $(1-r_u)$ is the ratio of flow in the disturbance waves to the total film flow rate.

Dispersion from a continuous point source

In the previous section mention was made of concentration measurements at points diametrically opposite and vertically above a point where a tracer was introduced continuously into the film. The measured concentration was shown to depend on the nature of the tracer which was interpreted as an ion fractionation effect.

The IDM may be adapted and solved under the boundary conditions and time invariance associated with these experimental conditions. The solution obtained for the concentration at points diametrically opposite the injection point and before tracer has spread round the column by circumferential diffusion is found to be (Roukens de Lange, 1975):

$$\frac{C_f}{C_m} \simeq \frac{1}{1-E+k_{if}E} + \frac{k_{if}}{(1-E)(1-E+k_{if}E)} \exp\left[\frac{-I(1-E+k_{if}E)Z}{(1-E)E}\right] - \frac{1}{1-E}\exp\left[\frac{-Ik_{if}Z}{1-E}\right] \qquad [7]$$

where C_m is the film concentration once the tracer has spread uniformly round the circumference. In deriving the equation, the effect of axial dispersion was ignored as its effect was negligible.

The above expression may in principle be used to estimate values for the parameters E, I and k_{if} from experimental values of C_f/C_m and Z (but see section 5). Several authors (Quandt 1965; Cousins & Hewitt 1968*b*; Jagota *et al.* 1973*a*) have used a similar technique to obtain estimates for E and I. All these authors injected a tracer continuously and uniformly around the tube circumference at a fixed height and measured concentration at downstream points in the film. The effect of ion fractionation was not considered in the analysis of these results.

Solution of the IDM for an impulse injection

The IDM model as given by [1a] and [1b] is similar to that obtained by Jagota *et al.* (1972), but allowance has been made for ion fractionation. These authors obtained solutions in terms of moments only. Although it did not prove possible to find a completely analytical solution, a solution was obtained in terms of a Fourier transform variable. Numerical solutions for C_f and C_d as functions of T and Z could then be found for any specified parameter values by the numerical inversion of the transformed expressions.

Experimental values for the parameters of the IDM may in principle be obtained by finding the parameter values which will give the model solution providing the best fit to the experimentally measured distribution. Such fits were carried out using a non-linear least-squares regression technique. The minimum least-squares solution was found using an algorithm developed by Powell (1964). The parameter values obtained in this manner and their validity will be discussed in the next section.

5. ANALYSIS OF EXPERIMENTAL RESULTS

Parameter values from least-squares fits

Before attempting to obtain experimental parameter values from least-squares fits of the IDM to measured concentration distributions, the sensitivity of the model solution to parameter values was tested. It was found that the solutions of the IDM were very insensitive to the parameters P_d and U_d/U_f. No attempt was therefore made to obtain values for these parameters and in all further analyses P_d was set equal to P_f while the ratio U_d/U_f was set at a value of 10. The parameters P_f, k_{if}, E and I all had significant influences on the shape of the concentration

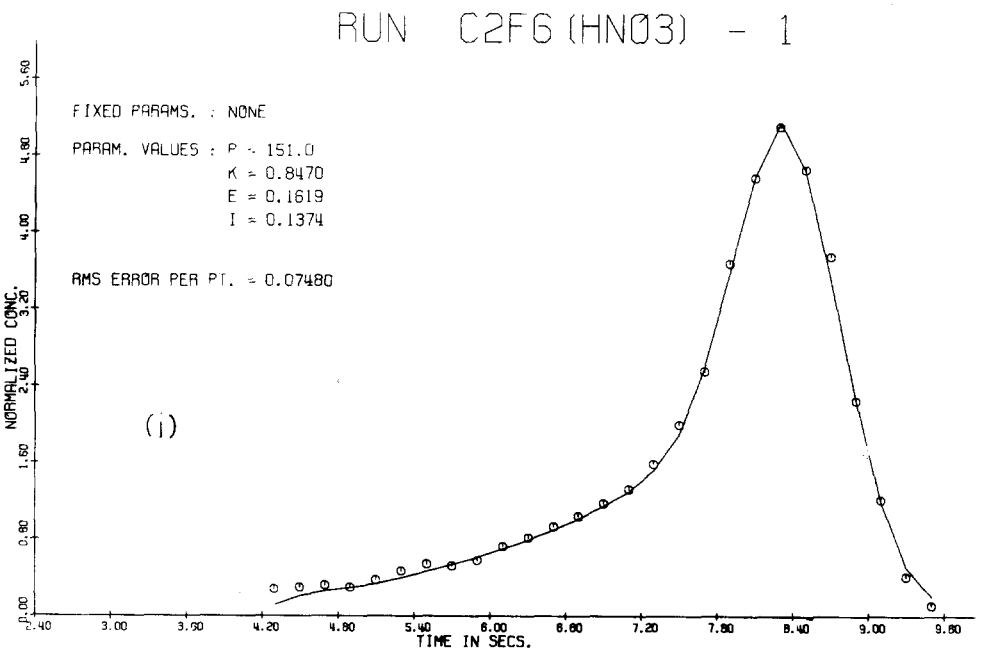

Figure 5(i)

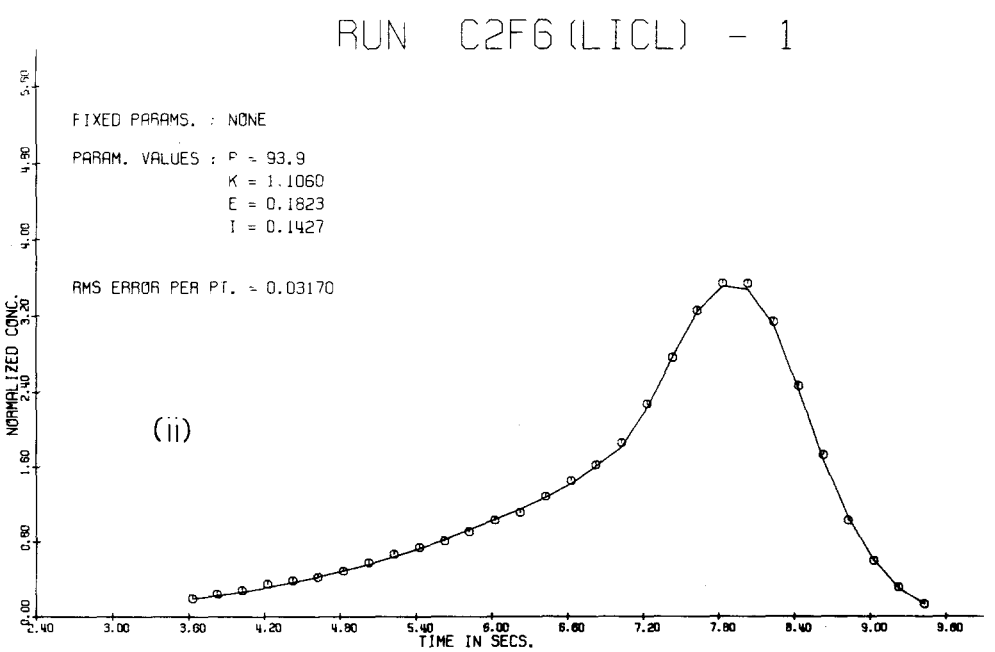

Figure 5(ii)

distributions for C_f and C_d. Parametric plots indicating these effects are given elsewhere (Roukens de Lange 1975; 1978).

Some typical least-squares fits to experimental concentration distribution data are given in figure 5. It can be seen that the fits are very good indeed. Unfortunately the agreement between parameter values for replicate runs was not very good and trends with liquid and gas flow rates were inconsistent. An investigation into the confidence contours in parameter space (see Draper & Smith 1966) indicated very wide confidence limits for the parameter estimates as a result of a high level of correlation between the effects of the various parameters on the concentration distribution.

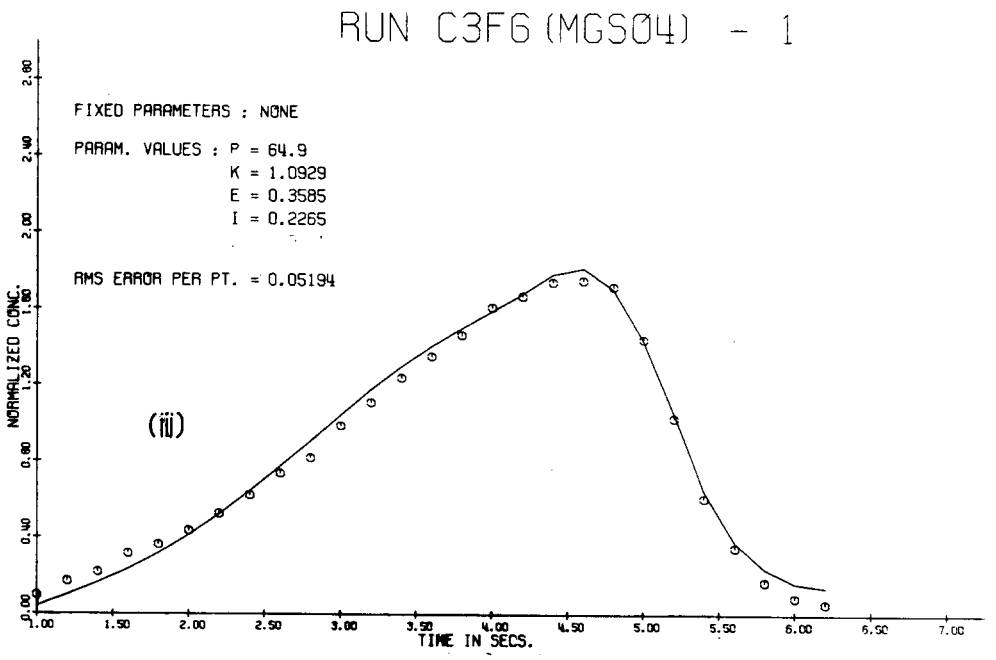

Figure 5(iii)

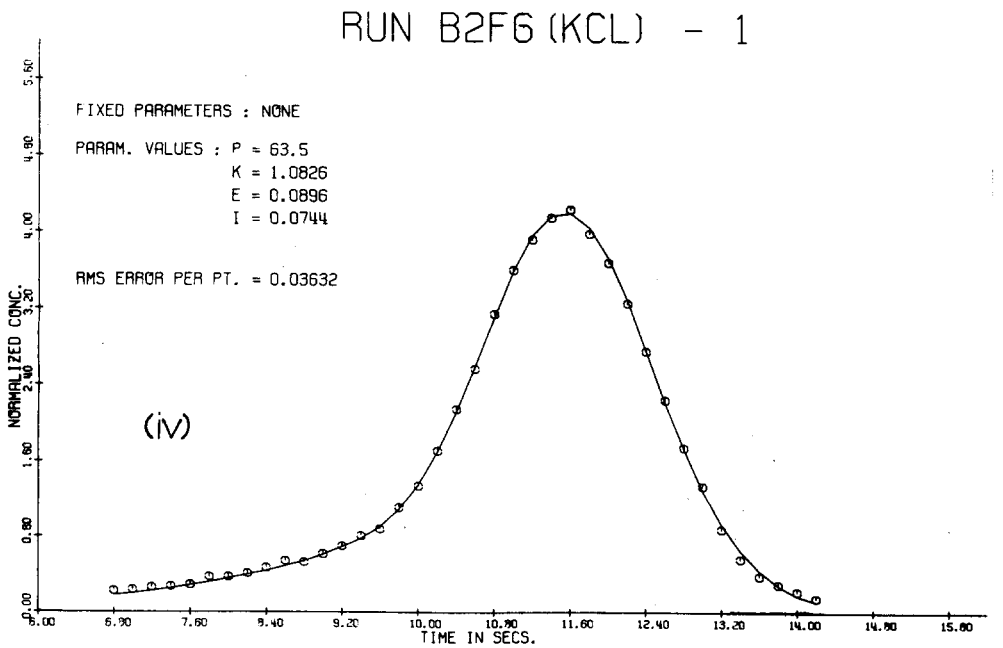

Figure 5(iv)

In order to extract useful information about parameters P_f and k_{if} the fitting procedure was repeated after fixing values for the tracer-independent parameters E and I for any given set of flow rates. As a result, confidence limits were improved by a factor of over 3 in the case of P_f and by a factor of about 40 in the case of k_{if}.

The values at which E and I were fixed were the means of values obtained when fitting all parameters. These values are of the same order as experimental values for E and I obtained by other investigators using different experimental techniques under similar experimental conditions (Jagota *et al.* 1973*a*,*b*; Cousins & Hewitt 1968*a*,*b*). The fixed values of E and I, though

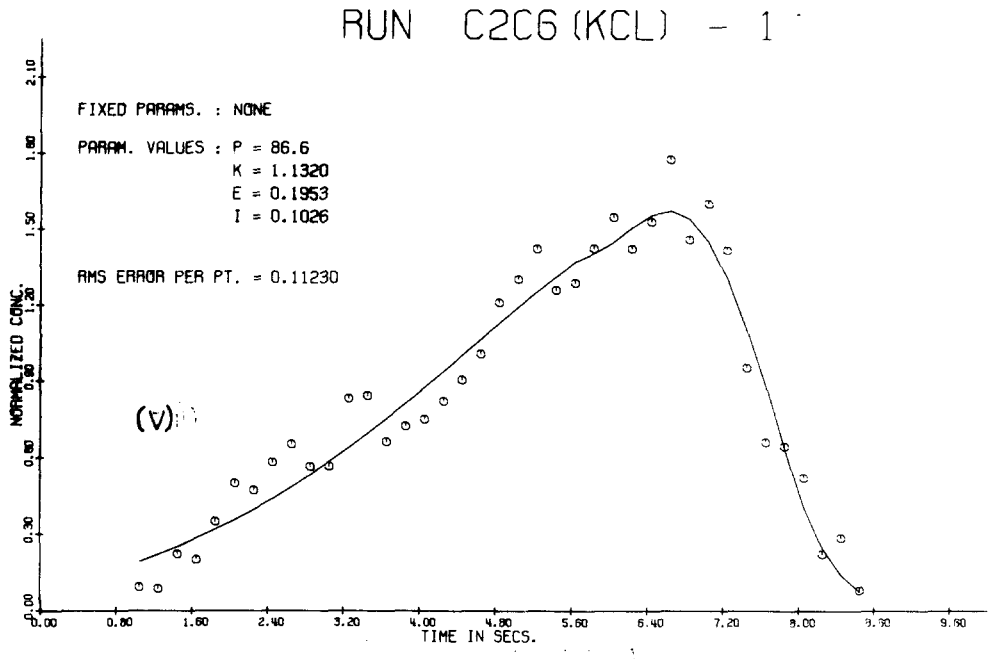

Figure 5(v)

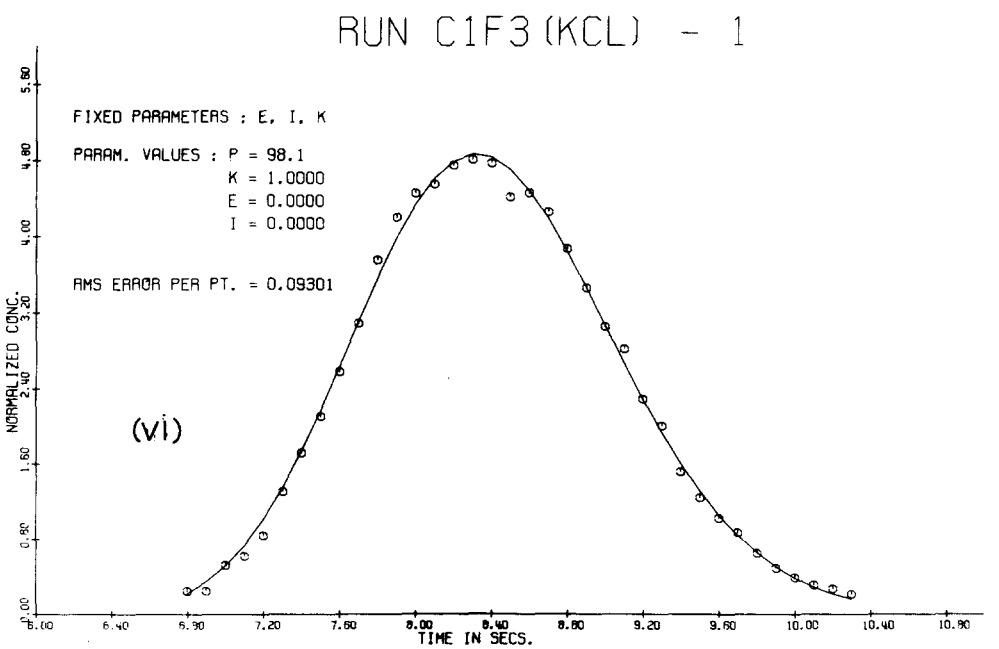

Figure 5(vi)

Figure 5. Examples of best-fit curves to experimental data.

consistent with the analysis, are not adequate for a meaningful comparison with the results of the other investigators.

A selection of results obtained for P_f and k_{if} using the above fitting procedure is presented in table 4. Not all the available experimental concentration distributions were fitted because of the large amount of computer time that would have been involved. Root mean square errors, e_{rms}, and computed mean film velocities, U_f, are also presented in table 4. Where available, values for e_{rms} obtained when fitting all parameters are also given. It can be seen that in most situations the quality of the fit is not seriously affected by fixing the two parameters.

A more complete analysis of dispersion in climbing film flow could have been achieved if independent experimental estimates had been available for the parameters E and I. As pointed out above such measurements have been made by other investigators, but their experimental techniques were not implemented. The only additional sources of information from which values of E and I may be obtained are those of dispersion in the core of continuous point injection experiments. The nature and quality of the data from these sources proved to be

Table 4. Results for the best fit of the IDM to some experimental concentration distributions. Parameters P_f and k_{if} are fitted; parameters E and I are fixed. The figures in brackets indicate the value of e_{rms} when all parameters are fitted.

Run	e_{rms}	P_f	k_{if}	u_f (m s^{-1})
[Experiment C2: $E = 0.1807$; $I = 0.1353$ m^{-1}]				
C2F6(HNO_3)—1	0.0980(0.0748)	145.2	0.817	0.697
C2F6(HNO_3)—2	0.0861	122.9	0.572	0.701
C2F6(HNO_3)—3	0.0790	120.4	0.605	0.704
C2F6(KOH)—1	0.1768	95.1	0.599	0.699
C2F6(KOH)—2	0.1249	94.6	0.658	0.698
C2F6(KOH)—3	0.0992	90.2	0.599	0.696
C2F6(KCl)—1	0.0573(0.0568)	88.9	1.069	0.704
C2F6(KCl)—2	0.0487(0.0429)	94.1	1.123	0.703
C2F6(KCl)—3	0.0473	80.2	1.032	0.713
C2F6(LiCl)—1	0.0346(0.0317)	93.0	1.156	0.720
C2F6(LiCl)—2	0.0487	95.1	1.240	0.710
C2F6(LiCl)—3	0.0421	88.2	1.217	0.707
C2F6($MgSO_4$)—1	0.0545(0.0529)	76.7	1.356	0.715
C2F6($MgSO_4$)—2	0.0615	74.0	1.219	0.722
C2F6($MgSO_4$)—3	0.0745	71.3	1.254	0.722
C2F3(KOH)—1	0.0483(0.0437)	93.2	0.868	0.721
C2F3(KCl)—1	0.0483	93.2	1.290	0.714
[Experiment C3: $E = 0.293$; $I = 0.226$ m^{-1}]				
C3F3(HNO_3)—1	0.0794(0.0614)	60.6	1.094	1.076
C3F3(KCl)—1	0.1096(0.0792)	55.0	1.417	1.047
C3F3($MgSO_4$)—1	0.1131(0.0951)	51.4	1.403	1.127
[Experiment B2: $E = 0.0850$; $I = 0.0770$]				
B2F6(HNO_3)—1	0.1200(0.1380)	85.6	0.550	0.500
B2F6(KCl)—1	0.0384(0.0363)	63.3	1.102	0.511
B2F6($MgSO_4$)—1	0.0648(0.0643)	52.9	1.057	0.512
[Experiment D2: $E = 0.339$; $I = 0.192$]				
D2F6(HNO_3)—1	0.0679(0.0674)	95.8	1.022	0.838
D2F6(KCl)—1	0.0576(0.0578)	92.0	1.028	0.802
D2F6($MgSO_4$)—1	0.0647(0.0618)	84.4	1.054	0.808
[Experiment C1: $E = 0$; $I = 0$]				
C1F6(KOH)—1	0.1552	110.9	—	0.367
C1F6(KCl)—1	0.1103	95.1	—	0.355
C1F6(LiCl)—1	0.2038	93.7	—	0.358
C1F6($MgSO_4$)—1	0.1272	80.7	—	0.358

inadequate for supplying satisfactory estimates for E and I (Roukens de Lange 1975).

In table 4 the results for Experiment C1 are obtained for $E = I = 0$. The reason for this is that at the low liquid rate of this experiment no disturbance waves and hence no entrainment occurred (Hewitt & Hall-Taylor 1970). In fact, a fit for all parameters indicated values for E and I close to zero. With E and I equal to zero the IDM reduces to a simple DPFM and this model was used to fit these concentration distributions. A typical fit obtained in this manner can be seen in figure 5(vi).

Results for the ion fractionation coefficient, k_{if}

Results for k_{if} obtained from fitting the IDM model to experimental results are summarised in table 5. Although the results are very scattered, it is clear that k_{if} is consistently higher for tracers KCl and $MgSO_4$ than for HNO_3.

Ion fractionation data can in principle be obtained from concentration measurements in a continuous point injection experiment. Unfortunately the experimental results given in table 3 do not correspond well with the relationship predicted by [7]. In figure 6 experimental and predicted values of concentration vs height are given. The theoretical curves were calculated using values for E, I and k_{if} given in tables 4 and 5. It can be seen that there is a difference in character between experimental and theoretical results. The rapid steepening of the experimental curves at large heights can probably be attributed to material moving around the circumference due to dispersion in the film itself. This conjecture was substantiated by injecting a dye continuously and observing its circumferential spreading. The initially slow rise in experimental concentration with height is probably due to the fact that entrained droplets are not homogeneously mixed as is assumed in deriving [7]. Presumably any droplet, after formation, will travel a finite distance with the gas stream before it can deposit on the opposite side of the tube. The trend of experimental results over the middle distance range appears to be in agreement with that predicted by theory in so far as higher concentrations for the ions Li^+, K^+ and Mg^{2+} than for H^+ are indicated.

Table 5. Values for k_{if} obtained by fitting experimental dispersion data at fixed values of E and I

Experiment	Tracer	Replicate runs fitted	k_{if}	$r_k = \frac{k_{if}}{k_{if}(HNO_3)}$
C2F6	HNO_3	3	0.665	—
C2F6	KOH	3	0.619	0.931
C2F6	KCl	3	1.075	1.617
C2F6	LiCl	3	1.204	1.811
C2F6	$MgSO_4$	3	1.276	1.918
C2F3	KOH	3	0.918	—
C2F3	KCl	3	1.304	—
C3F6	HNO_3	1	0.900	—
C3F6	KCl	1	1.348	1.498
C3F6	$MgSO_4$	1	1.331	1.477
C3F3	HNO_3	1	1.094	—
C3F3	KCl	1	1.417	1.294
C3F3	$MgSO_4$	1	1.403	1.283
B2F6	HNO_3	1	0.550	—
B2F6	KCl	1	1.102	2.004
B2F6	$MgSO_4$	1	1.057	1.921
B2F3	HNO_3	1	0.980	—
B2F3	$MgSO_4$	1	1.008	1.092
D2F6	HNO_3	1	1.022	—
D2F6	KCl	1	1.028	1.006
D2F6	$MgSO_4$	1	1.054	1.032
D2F3	HNO_3	1	1.012	—
D2F3	KCl	1	1.472	1.453
D2F3	$MgSO_4$	1	1.551	1.530

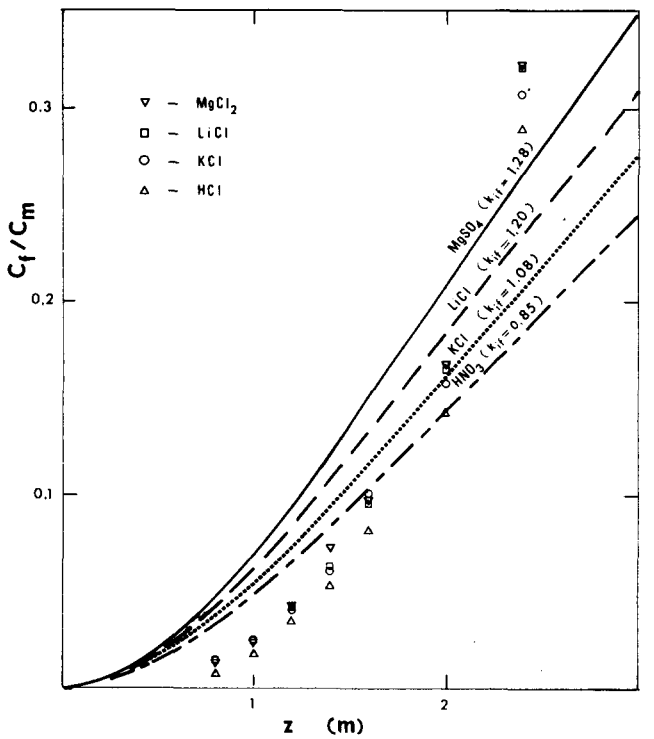

Figure 6. Concentration as a function of height above, and diametrically opposite, a continuous injection point. Points represent experimental values. Curves represent concentrations calculated from [7] using parameter values corresponding to mean experimental values for Experiment C2 ($E = 0.1807$; $I = 0.1353$; k_{if} as indicated on curves).

Trend analysis for the dispersion parameter, P_f

The results for P_f in table 4 clearly indicate an effect due to the tracer. Equation [3], which was developed on the assumption of the existence of a viscous sub-layer, indicates that a plot of $1/P_f$ against P_{mol} (or $1/D_{mol}$) should, for a given set of flow conditions, result in a linear relationship. Data obtained for Experiments C1 and C2 are plotted for such axes in figure 7. The best-fit linear regression lines and confidence limits are also indicated. It can be seen that the linear relationship for Experiment C2 is not very good and, in fact, a test for lack of fit indicated a deviation from linearity significant at the 99.9% level. It might at first be thought that the deviation from linearity indicates an inadequacy in the viscous sub-layer model. However, if this were the case, the deviation should be a smooth function of molecular diffusivity. Instead, deviations appear to be associated with individual tracer materials. The effect cannot be interpreted simply in terms of ion enrichment at the interface and no other obvious explanation can be offered (Roukens de Lange 1975).

Despite the unexplained deviations from the simple linear relationship predicted by [3], no evidence has emerged which is in conflict with the assumption of the existence of a viscous sub-layer. Using values for the slope and intercept for the best linear fit as indicated in figure 7, and making the necessary substitutions of experimental values in [3–5], values for y_v may be found by solution of the implicit [4]. Values for the contribution to dispersion due to the remainder of the film, P_t, were obtained from the intercept. Results are given in table 6.

The parameter P_t reflects the combined effects of all other sources of dispersion. Equation [6], which was developed on the basis of a simple theory of disturbance waves mixing with a base film in viscous flow, allows values of P_t to be calculated. In table 7 values for P_t calculated from [6] are given. Experimental values for P_t and quantities required in the calculation of P_t are also given. It can be seen that calculated and experimental values for P_t are of the same

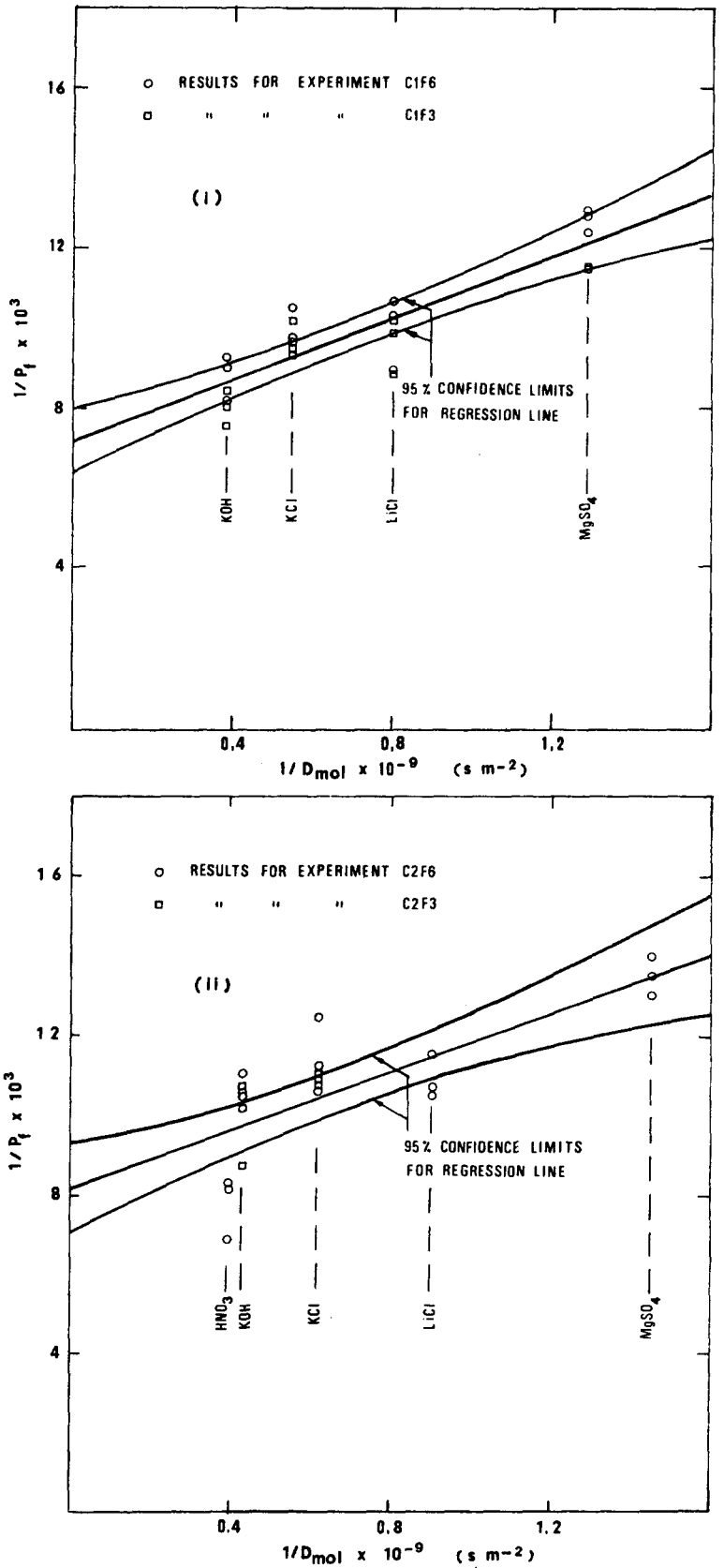

Figure 7. Linear least-squares fit for the relationship between the dispersion parameter, P_f, and molecular diffusivity, D_{mol}.

Table 6. Results for viscous wall layer thickness, y_v, and turbulent layer dispersion parameter, P_t

Experiment	C1	C2
$y_i(m \times 10^6)$	127	157
$y_v(m \times 10^6)$	7.63	7.30
P_t	135	119

Table 7. Data for calculating values for the turbulent dispersion parameter, P_t

Experiment	u_m ($m\,s^{-1}$)	U_f	U_t	F_w	r_u	P_t (calc.)	P_t (exptl.)
C1	0.357	1.000	1.038	—	—	—	135
C2	0.886	0.801	0.824	8.92	0.90	107	119
C3	1.623	0.678	0.698	8.08	0.63	123	63
B2	0.555	0.908	0.935	10.27	0.84	83	96
D2	1.272	0.801	0.825	8.17	0.95	79	100

order of magnitude. Considering the complex nature of climbing film flow, better agreement could hardly have been expected.

It should be noted that results for Experiment C1 indicate that turbulence and mixing in the film are not caused solely by disturbance waves. Experiment C1 was carried out at a liquid flow rate below that for which disturbance waves appear, yet the effect of molecular diffusivity on the overall dispersion coefficient is small [see figure 7(i)], indicating considerable turbulence penetrating deeply into the film. This observation can only be explained if ripple waves are assumed to cause a significant degree of mixing.

6. INTERFACIAL TURBULENCE AND HEAT TRANSFER

Data on liquid transported by disturbance waves (Hewitt & Nicholls 1969) and entrained droplets (Gill *et al.* 1964) can be used to show that the flow rate of liquid in the "base film" does not vary greatly with total liquid rate, and that the Reynolds numbers of 300–600 associated with flow in this layer lie well within the viscous flow regime (Roukens de Lange 1975). In attempting to interrelate liquid flow rate, film thickness and pressure gradient in climbing film flow, many authors have assumed that the turbulance found in climbing film flow is frictional turbulence similar to that found in full pipe flow at high Reynolds numbers (Calvert & Williams 1955; Anderson & Mantzouranis 1960; Hewitt 1961; Davies 1965). However this assumption must clearly be invalid and the turbulence in climbing film flow is in fact interfacial turbulence. A number of authors, e.g. Willis (1965) and Hewitt & Hall-Taylor (1970) have indicated their awareness of this fact. It is rather surprising that in spite of its unsatisfactory physical basis, the frictional turbulence theory has proved very effective in correlating film thickness data (Gill *et al.* 1964). However, Ueda & Nose (1974) have found that heat transfer data cannot be satisfactorily correlated by this theory.

The findings of the present investigation suggest that heat transfer data might be correlated if it is assumed that the heat passes by conduction through a viscous layer of negligible thermal capacity before being instantaneously and uniformly distributed in a radial direction as a result of interfacial turbulence. The heat transfer coefficient would therefore be given by $h = k y_v$ where k is the thermal conductivity of the liquid. Results for heat transfer to a climbing water film obtained by Ueda & Nose (1974), and Penman and Tait (1965), when analysed in this manner, indicate values for y_v in the range 50–100 μm. Actual values for y_v were seen in table 6 to be an order of magnitude smaller. This simple model for heat transfer to climbing films therefore has no validity. The probable reason for the failure of this interpretation is that while the base film is viscous for most of the time, for a small proportion of the time turbulence will

penetrate to within, say, 10 μm of the wall, presumably as a result of a wave passing over the interface. Thus the level of turbulence varies greatly with time. The effect of the essentially viscous nature of the base film is strong in the case of heat transfer because transfer is in a radial direction. On the other hand, the periodic turbulence will not allow molecular dispersion patterns to develop as dispersion takes place in an axial direction. The only observable molecular effect will be due to the very thin layer next to the wall where turbulence generated at the interface does not penetrate. This layer is the effective viscous sub-layer for which calculated values are given in table 6.

7. CONCLUSIONS

In this investigation the nature of dispersion in climbing film flow was investigated by measuring concentration distributions resulting from tracer injections. The experimental results were analysed in terms of mathematical models based on the physical mechanisms of dispersion. The major findings of the investigation are summarised below.

(i) In climbing film flow the major factors determining dispersion are interchange of material between the film and entrained droplets in the gas core, velocity profile in the film, turbulence created at the gas–liquid interface and transport in disturbance waves.

(ii) Dispersion in climbing film flow is affected by the nature of the tracer. A very thin viscous sub-layer next to the tube wall, approx 5–10 μm thick, makes a small contribution which is dependent on the molecule diffusivity of the tracer. It also appears that tracer material concentrates at the gas–liquid interface in an unexplained manner and to an extent dependent on the nature of the tracer. This creates a concentration effect in droplets formed at the interface known as "ion fractionation".

(iii) The dispersion in the film itself, i.e. not including the effect of interaction with the entrained phase, can be described in terms of a dispersed plug flow model (DPFM). The dispersion parameter, P_f, can be expressed as a composite function of the various dispersive effects occurring in the film.

(iv) The observed pattern of dispersion in the film, i.e. including the effect of interaction with the entrained phase, can be described very effectively in terms of an interchange dispersion model (IDM). This model can also account for the dispersion pattern observed in the entrained liquid. The shape of the dispersion patterns is described in terms of four principal parameters: the film dispersion parameter, P_f; the ion fractionation coefficient, k_{if}; the fractional entrainment, E; and the fractional liquid interchange per unit length of tube, I.

(v) Because of correlation between the effects of the above parameters on the measured concentration distribution it is not possible to obtain reliable values for all four parameters by a least-squares fit of the IDM. However, if E and I are fixed for a given set of flow conditions, reasonably consistent values for P_f and k_{if} can be found.

(vi) The liquid rate in the base film corresponds to Reynolds numbers in the range 300–600, well within the region of viscous flow. The rest of the liquid is carried up as disturbance waves or entrained droplets. Turbulence in the film is therefore not like that found at high Reynolds numbers in full pipe flow but results from disturbances generated at the gas–liquid interface by ripple waves or the passage of disturbance waves over the base film. Heat transfer correlations based on the concepts of frictional turbulence in full pipe flow fail to interpret experimental results.

Acknowledgements—The author would like to express his gratitude to Professor D. Glasser, who supervised the research and who provided much useful advice and encouragement. The financial assistance of The Council for Scientific and Industrial Research is also acknowledged gratefully.

REFERENCES

ANDERSON, G. H. & MANTZOURANIS, B. G. 1960 Two-phase gas–liquid flow phenomena: I. Pressure drop and hold-up for two-phase flow in vertical tubes. *Chem. Engng Sci.* **12**, 109–126.

ARIS, R. 1956 On the dispersion of a solute in a fluid flowing through a tube. *Proc. R. Soc. Lond.* A. **235**, 67–77.

CALVERT, S. & WILLIAMS, B. 1955 Upward co-current annular flow of air and water in smooth tubes. *A.I.Ch.E.J.* **1**, 78.

COUSINS, L. B. & HEWITT, G. F. 1968*a* Liquid phase mass transfer in annular two-phase flow: radial liquid mixing. AERE R-5693.

COUSINS, L. B. & HEWITT, G. F. 1968*b* Liquid phase mass transfer in annular two-phase flow: droplet deposition and liquid entrainment. AERE R-5657.

DAVIES, E. J. 1965 An analysis of liquid film flow. *Chem. Engng Sci.* **20**, 265–272.

DRAPER, N. R. & SMITH, H. 1966 *Applied Regression Analysis.* Wiley, New York.

GREEN, R. 1973 A portable multi-channel seismic recorder and a data processing system. *Bull. Seism. Soc. Am.* **63**, 423–431.

GILL, L. E., HEWITT, G. F. & LACEY, P. M. C. 1964 Sampling probe studies of the gas core in annular two-phase flow: II, Studies of the effect of phase flowrates on phase and velocity distribution. *Chem. Engng Sci.* **19**, 665–682. See also AERE R-3955, 1963.

GILL, W. N. & SANKARASUBRAMAMIAN, R. 1971. Dispersion of a non-uniform slug in time-dependent flow. *Proc. R. Soc. Lond.* A. **322**, 101–117.

HEWITT, G. F. 1961 Analysis of annular two-phase flow; application of the Dukler analysis to vertical upward flow in a tube. AERE-R 3680, H.M.S.O.

HEWITT, G. F. 1969 Disturbance waves in annular two-phase flow. In *Fluid Mechanics and Measurements in Two-Phase Flow Systems*, Proc. Instn Mech. Engrs **184**, Part 3C, 142–150.

HEWITT, G. F. & HALL-TAYLOR, N. S. 1970 *Annular Two-phase Flow.* Pergamon Press, Oxford.

HEWITT, G. F., KING, R. D. & LOVEGROVE, P. C. 1964 Techniques for liquid film and pressure drop studies in annular two-phase flow. *Chem. Process Engng* **45**, 191.

HEWITT, G. F. & NICHOLLS, B. 1969 Film thickness measurements in annular two-phase flow using a fluorescence spectrometer technique. Part II: Studies of the shape of disturbance waves. AERE-R 4506.

JAGOTA, A. K., SCOTT, D. S. & RHODES, E. 1972 Radial mixing and residence times in the liquid phase in gas–liquid annular flow in vertical tubes. *Can. J. Chem. Engng* **50**, 194–203.

JAGOTA, A. K., RHODES, E. & SCOTT, D. S. 1973*a* Tracer measurements in two-phase annular flow to obtain interchange and entrainment. *Can. J. Chem. Engng* **51**, 139–147.

JAGOTA, A. K., RHODES, E. & SCOTT, D. S. 1973*b* Measurement of residence times, and film and drop velocities in two-phase annular flow. *Can. J. Chem. Engng* **51**, 393–399.

MACINTYRE, F. 1972 Flow patterns in breaking bubbles. *J. Geophys. Res.* **77**, 5211–5228.

MACINTYRE, F. 1974 The top millimeter of the ocean. *Scient. Am.* **230**(5), 62–77.

PENMAN, T. O. & TAIT, W. F. 1965 Heat transfer in liquid-film flow. *IEC Fundamentals* **4**, 407–416.

POWELL, M. J. D. 1964 An efficient method for finding the minimum of a function of several variables without calculating derivatives. *Computer J.* **7**, 155–162.

QUANDT, E. R. 1965 Measurement of some basic parameters in two-phase annular flow. *A.I.Ch.E.J.* **11**, 311–318.

ROBERTS, D. N. 1969 The Lotus (Long Tube System) air–water loop design and description. AERE-M 2175.

ROUKENS DE LANGE, A. 1975 *Dispersion in annular climbing film flow.* Ph.D. Thesis, University of the Witwatersrand.

ROUKENS DE LANGE, A. 1978 Dispersion models for annular climbing film flow. *Appl. Math. Model.* **2**, 99–108.

TAYLOR, Sir G. I. 1953 Dispersion of soluble matter in solvent flowing slowly through a tube. *Proc. R. Soc. Lond.* A. **219**, 186–203.

UEDA, T. & NOSE, S. 1974 Studies of liquid film flow in two-phase annular and annular-mist flow regions. *Bull. J.S.M.E.* **17**, 614–624.

WILLIS, I. J. 1965 Upwards annular two-phase air/water flow in vertical tubes. *Chem. Engng Sci.* **20**, 895–902.